



ELSEVIER

Contents lists available at ScienceDirect

## Journal of Sound and Vibration

journal homepage: [www.elsevier.com/locate/jsvi](http://www.elsevier.com/locate/jsvi)

# Natural mode analysis of an acoustic cavity with multiple elliptical boundaries by using the collocation multipole method

W.M. Lee\*

Department of Mechanical Engineering, China University of Science and Technology, Taipei, Taiwan

## ARTICLE INFO

## Article history:

Received 18 June 2010

Received in revised form

11 February 2011

Accepted 1 May 2011

Handling Editor: L.G. Tham

Available online 31 May 2011

## ABSTRACT

This paper presents a semi-analytical approach to solve the eigenproblem of an acoustic cavity with multiple elliptical boundaries. To satisfy the Helmholtz equation in the elliptical coordinate system, the multipole expansion for the acoustic pressure is formulated in terms of angular and radial Mathieu functions. The boundary conditions are satisfied by uniformly collocating points on the boundaries. The acoustic pressure at each point is directly calculated in each elliptical coordinate system. In different coordinate systems, the normal derivative of the acoustic pressure is calculated by using the appropriate directional derivative, an alternative to the addition theorem. By truncating the multipole expansion, a finite linear algebraic system is derived. The direct searching approach is employed to determine the natural frequencies by using the singular value decomposition (SVD). Numerical results are widely discussed for several examples including an elliptical cavity, a confocal elliptical annulus cavity and an elliptical cavity with two elliptical cylinders. The accuracy and numerical convergence of the presented method is validated by comparison with available results from the analytical method and the commercial finite-element code ABAQUS. No spurious eigensolutions are found in the proposed formulation. Excellent accuracy and fast rate of convergence are the key features of the present method thanks to its semi-analytical feature.

© 2011 Elsevier Ltd. All rights reserved.

## 1. Introduction

The natural mode analysis of an acoustic cavity can provide important information in the design phase for the cavity related to mechanical systems such as automobile mufflers and hermetic compressors [1]. Although the natural mode for the cavities other than circular sections can be obtained by using the finite element method (FEM) or the boundary element method (BEM) [2], analytical solutions, if available, usually result in accurate and fast rate convergence methodologies and provide the physical insight to the considered problem. A semi-analytical approach to the eigenproblem for an acoustic cavity with elliptical boundaries is presented in this paper.

Over the past few decades, most of the analytical solutions for natural modes have focused on the simple geometries such as circular or annular cavities [3–6]. However, except Ref. [1], no attention has been focused on acoustic problems involving elliptical boundaries, probably because its formulation involves the ill-familiar and complicated Mathieu functions [7–12]. Hong and Kim [1] analytically derived the characteristic equations of both hollow and annular elliptical cylindrical cavities in terms of Mathieu functions and presented the circular cylinders as a special case of their results. Chen et al. [5–6] applied the

\*Tel.: +886 2 2786 7048x26; fax: +886 2 2786 7253.

E-mail address: [wmllee@cc.cust.edu.tw](mailto:wmllee@cc.cust.edu.tw)

null-field boundary integral equation method (BIEM) to solve the eigenproblems with circular boundaries. Recently, Chen et al. extend the BIEM to deal with torsion problems containing multiple elliptical inclusions [13] and eigenproblems of a confocal elliptical membrane [14], performing an analytical investigation of spurious eigenvalues and providing several remedies to suppress them. It is well known that the BIEM (or BEM) belongs to the boundary-type method which can reduce the dimension of the original problem by one. Consequently the number of the unknowns is much less than that of the domain type methods such as the FEM. In addition, the domain mesh generation is not required, which is generally the most difficult and time consuming task. However, the boundary integration is required in the BIEM and spurious eigenvalues always occur for multiply-connected domain problems even though they can be suppressed by using complex kernel functions for simply-connected domain problems. Hence a formulation with no integration and no spurious eigenvalues is our concern. The spurious eigenvalues stem from the non uniqueness of solution. Specifically, spurious eigenvalues arise from the incomplete solution representation such as the real-part BEM, multiple reciprocity method. In this paper, the even and odd angular and radial Mathieu functions are employed to represent the acoustic field.

The concept of multipole method to solve multiply-connected domain problems was introduced by Závřiska [15] and used to deal with the interaction of waves with arrays of circular cylinders by Linton and Evans [16]. For applications of the multipole method to acoustic problems, readers may consult with a recent monograph by Martin [17]. The addition theorem is often employed to transform the multipole expansion into one of coordinate systems to satisfy the specified boundary conditions. For the circular boundary, some applications can be seen in the water wave scattering problem [16], the free vibration of circular membranes [18,19], the free vibration of circular plates [19,20] and the flexural wave scattering [21]. Furthermore, Chatjigeorgiou and Mavrakos [22,23] proposed an analytical approach to the hydrodynamic diffraction by multiple elliptical cylinders using the addition theorem of the Mathieu functions derived from Graf's addition theorem for the Bessel functions. In the view point of mathematics, the procedure is elegant. But we need to face the complicated formulation and the accompanying numerical calculation due to the infinite series form of the addition theorem for Mathieu functions so that its applications are limited.

This paper presents a semi-analytical approach to the eigenproblem for an acoustic cavity with multiple elliptical boundaries. To satisfy the Helmholtz equation in the elliptical coordinate system, the proper Mathieu functions are chosen to formulate the acoustic pressure caused by outer elliptical cavity and inner elliptical boundaries, respectively. By uniformly collocating points on the boundaries, the normal derivative of acoustic pressure at the collocation point is exactly calculated by using directional derivative in each coordinate system to satisfy the Neumann boundary condition (or sound-hard conditions) as an alternative to the addition theorem. In this way, a coupled infinite system of simultaneous linear algebraic equations is derived. Based on the direct searching approach [24], the nontrivial eigensolutions can be determined by finding the zero determinant of the truncated finite system through the technique of singular value decomposition (SVD). After determining the unknown coefficients of the multipole expansion, the corresponding natural modes can be obtained. Several numerical examples are presented and the proposed results of an elliptical cavity, a confocal elliptical annulus cavity and an elliptical cavity with two elliptical cylinders are compared with those of the available analytical solutions and the ABAQUS FEM solver [25]. Since BIEM or BEM results in spurious eigenvalues for multiply-connected domain problems, the appearance of spurious solution by using the present method will be examined here.

## 2. Problem statement and the general solution in the elliptical coordinate system

A two-dimensional elliptical cavity with  $H$  nonoverlapping elliptical cylinders has a domain  $\Omega$  which is enclosed with boundary,

$$B = \bigcup_{j=1}^L B_j, \quad (1)$$

as shown in Fig. 1, where  $O_j$  and  $B_j$  denote the center of the  $j$ th ellipse and its boundary, the subscript  $j=1, \dots, L$  ( $L=1+H$  and  $O_1$  is the center of the outer elliptical cavity). We will use  $L+1$  observer coordinate systems:  $(z_1, z_2)$  is a global Cartesian coordinate system centered at  $O$ ;  $(\xi_j, \eta_j)$ ,  $j=1, \dots, L$  is the  $j$ th local elliptical coordinate system centered at  $O_j$  with global Cartesian coordinates  $(z_1^j, z_2^j)$ . The major and minor semi axes of  $j$ th ellipse are  $a_j$  and  $b_j$ , respectively, and its local coordinate system makes an angle  $\theta_j$  with respect to the global coordinate system. The governing equation for an acoustic cavity is the Helmholtz equation:

$$(\nabla^2 + k^2)P(\mathbf{x}) = 0, \quad \mathbf{x} \in \Omega, \quad (2)$$

where  $\nabla^2$  is the Laplace operator,  $P$  is the acoustic pressure,  $k=\omega/c$  is the wavenumber,  $\omega$  is the radian frequency,  $c$  is the speed of sound in the acoustic medium and  $\mathbf{x}$  is a typical field point in the domain  $\Omega$ .

To properly deal with the geometry considered in this paper, the elliptical coordinate system [7–12] as shown in Fig. 2 should be used. The elliptical coordinates  $(\xi, \eta)$  are related to the rectangular coordinates  $(x, y)$  by the relation

$$x + iy = f \cosh(\xi + i\eta), \quad (3)$$

where  $i = \sqrt{-1}$ ,  $\xi$  is a radial coordinate ( $\xi \geq 0$ ),  $\eta$  is an angular coordinate ( $0 \leq \eta < 2\pi$ ) and  $2f$  is the interfocal distance.

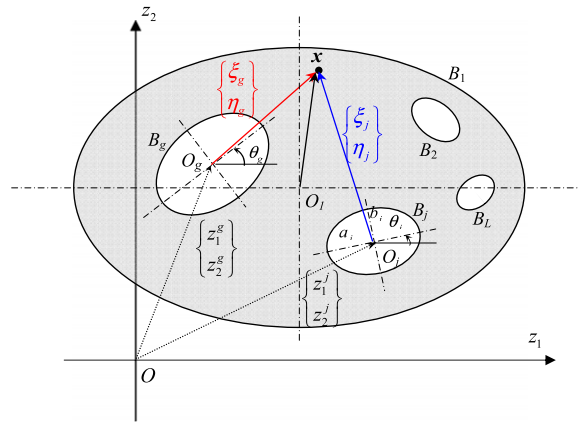


Fig. 1. Problem statement for an acoustic cavity with multiple elliptical boundaries.

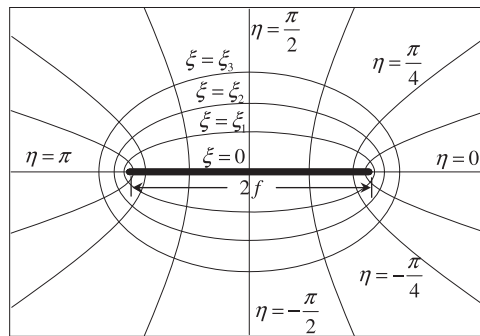


Fig. 2. Elliptical coordinate system.

Separating and equating real and imaginary parts of Eq. (3) give

$$x = f \cosh \xi \cos \eta, \quad y = f \sinh \xi \sin \eta. \tag{4}$$

The coordinate curves constructed by orthogonally intersecting confocal ellipses ( $\xi = \text{constant}$ ) and hyperbolas ( $\eta = \text{constant}$ ) are illustrated in Fig. 2. In the elliptical coordinate system with the inter-focal distance  $2f$ , an ellipse can be easily described by a fixed radial variable, for example  $\xi = \xi_0$ , where the half-lengths of major and minor axes, respectively, are obtained by

$$a = f \cosh \xi_0, \quad b = f \sinh \xi_0. \tag{5}$$

The eccentricity of an ellipse is given by

$$e = 1 / \cosh \xi_0 = f / a. \tag{6}$$

On the other hand, when the major and minor axes are given, the corresponding radial coordinate and the inter-focal distance can be obtained by

$$\xi_0 = \tanh^{-1}(b/a), \quad f = a / \cosh \xi_0. \tag{7}$$

In the elliptical coordinate system, using the transformation of Eq. (4), the Helmholtz equation of Eq. (2) takes the form

$$\frac{1}{h} \left( \frac{\partial^2 P(\xi, \eta)}{\partial \xi^2} + \frac{\partial^2 P(\xi, \eta)}{\partial \eta^2} \right) + k^2 P(\xi, \eta) = 0, \tag{8}$$

where the scaling factor  $h$  is given by one of the following expressions [9]:

$$f \sqrt{\sinh^2 \xi + \sin^2 \eta}, \quad f \sqrt{\cosh^2 \xi - \cos^2 \eta} \quad \text{and} \quad f \sqrt{\cosh 2\xi - \cos 2\eta} / \sqrt{2}.$$

By using the method of separation variables,

$$P(\xi, \eta) = R(\xi)\Phi(\eta). \tag{9}$$

Eq. (8) results in

$$\frac{\partial^2 \Phi(\eta)}{\partial \eta^2} + (\sigma - 2q \cos 2\eta)\Phi(\eta) = 0, \tag{10}$$

$$\frac{\partial^2 R(\xi)}{\partial \xi^2} - (\sigma - 2q \cosh 2\xi)R(\xi) = 0, \tag{11}$$

where  $q = (fk/2)^2$  and  $\sigma$  are the separation constants. Eqs. (10) and (11) are known as the Mathieu equation and the modified Mathieu equation, or the angular Mathieu equation and the radial Mathieu equation. For given no zero  $q$ , we can determine the eigenvalues  $\sigma$  and their solutions called the even and the odd angular Mathieu functions, respectively, denoted by

$$\Phi_m = \begin{cases} ce_m(\eta, q), & m = 0, 1, 2, \dots, \\ se_m(\eta, q), & m = 1, 2, \dots \end{cases} \tag{12}$$

and the even and the odd radial Mathieu functions of the first kind and the second kind, respectively, denoted by

$$R_m = \begin{cases} Mc_m^{(1)}(\xi, q), & Mc_m^{(2)}(\xi, q), & m = 0, 1, 2, \dots \\ Ms_m^{(1)}(\xi, q), & Ms_m^{(2)}(\xi, q) & m = 1, 2, \dots \end{cases} \tag{13}$$

Analogous to the Hankel functions in the case of the Bessel functions, the even and the odd radial Mathieu functions of the third kind and the fourth kind, respectively, are defined by

$$\begin{aligned} Mc_m^{(3),(4)}(\xi, q) &= Mc_m^{(1)}(\xi, q) \pm iMc_m^{(2)}(\xi, q), & m = 0, 1, 2, \dots \\ Ms_m^{(3),(4)}(\xi, q) &= Ms_m^{(1)}(\xi, q) \pm iMs_m^{(2)}(\xi, q), & m = 1, 2, \dots \end{aligned} \tag{14}$$

From Eqs. (12)–(14), in the elliptical coordinates, the Helmholtz equation has separated solutions of the form

$$Mc_m^{(i)}(\xi, q)ce_m(\eta, q) \quad \text{and} \quad Ms_m^{(i)}(\xi, q)se_m(\eta, q), \quad i = 1, 2, 3 \text{ and } 4.$$

It is noted that the corresponding angular and radial Mathieu functions in each product have the same eigenvalue  $\sigma$ . Since the product  $Mc_m^{(2)}(\xi, q)ce_m(\eta, q)$  does not satisfy the continuity in gradient across the interfocal line and the product  $Ms_m^{(2)}(\xi, q)se_m(\eta, q)$  does not satisfy the function continuity [9], the permissible solution of Eq. (2) is

$$P^I(\xi, \eta) = \sum_{m=0}^{\infty} c_m Mc_m^{(1)}(\xi, q)ce_m(\eta, q) + \sum_{m=1}^{\infty} s_m Ms_m^{(1)}(\xi, q)se_m(\eta, q) \tag{15}$$

for the interior domain to the elliptical boundary, where the coefficients  $c_m$  and  $s_m$  are to be determined by the boundary conditions, and

$$P^E(\xi, \eta) = \sum_{m=0}^{\infty} c_m Mc_m^{(3)}(\xi, q)ce_m(\eta, q) + \sum_{m=1}^{\infty} s_m Ms_m^{(3)}(\xi, q)se_m(\eta, q) \tag{16}$$

for the exterior domain, which satisfies the radiation condition at infinity.

### 3. The multipole method

The problem of an elliptical cavity with  $H$  elliptical cylinders can be decomposed into one interior domain problem and  $H$  exterior domain problems. For this multiply-connected domain problem, using Eqs. (15) and (16), the acoustic pressure satisfying Eq. (2) can be explicitly expressed as an infinite sum of multipoles at the center of each ellipse

$$\begin{aligned} P(\mathbf{x}; \xi_1, \eta_1, \xi_2, \eta_2, \dots, \xi_L, \eta_L) &= c_0^1 Mc_0^{(1)}(\xi_1, q)ce_0(\eta_1, q) \\ &+ \sum_{m=1}^{\infty} c_m^1 Mc_m^{(1)}(\xi_1, q)ce_m(\eta_1, q) + s_m^1 Ms_m^{(1)}(\xi_1, q)se_m(\eta_1, q) + \sum_{j=2}^L \left[ c_0^j Mc_0^{(3)}(\xi_j, q)ce_0(\eta_j, q) \right. \\ &\left. + \sum_{m=1}^{\infty} c_m^j Mc_m^{(3)}(\xi_j, q)ce_m(\eta_j, q) + s_m^j Ms_m^{(3)}(\xi_j, q)se_m(\eta_j, q) \right] \end{aligned} \tag{17}$$

and the normal derivative of the acoustic pressure, appearing in the sound-hard or Neumann boundary condition, is expressed as

$$\begin{aligned} \frac{\partial}{\partial n} P(\mathbf{x}; \xi_1, \eta_1, \xi_2, \eta_2, \dots, \xi_L, \eta_L) &= c_0^1 \frac{\partial}{\partial n} (Mc_0^{(1)}(\xi_1, q)ce_0(\eta_1, q)) \\ &+ \sum_{m=1}^{\infty} c_m^1 \frac{\partial}{\partial n} (Mc_m^{(1)}(\xi_1, q)ce_m(\eta_1, q)) + s_m^1 \frac{\partial}{\partial n} (Ms_m^{(1)}(\xi_1, q)se_m(\eta_1, q)) \\ &+ \sum_{j=2}^L \left[ c_0^j \frac{\partial}{\partial n} (Mc_0^{(3)}(\xi_j, q)ce_0(\eta_j, q)) + \sum_{m=1}^{\infty} c_m^j \frac{\partial}{\partial n} (Mc_m^{(3)}(\xi_j, q)ce_m(\eta_j, q)) + s_m^j \frac{\partial}{\partial n} (Ms_m^{(3)}(\xi_j, q)se_m(\eta_j, q)) \right], \end{aligned} \tag{18}$$

where  $\xi_j$  and  $\eta_j$  ( $j=1, 2, \dots, L$ ) denote the elliptical coordinates of the field point  $\mathbf{x}$  with respect to the  $j$ th local elliptical coordinate system. The coefficients  $c_m^j$  and  $s_m^j$  can be determined by the boundary conditions. The normal derivative can be easily expressed by  $\partial/\partial\xi$  when the field point on the boundary of an ellipse is described by its local elliptical coordinate system. In the next section, the more complex evaluation of the normal derivative on a boundary described by non-local elliptical coordinates will be discussed.

To determine these unknown coefficients, the calculation of both Eqs. (17) and (18) is needed. But this procedure involves the derivative of multivariable functions and this is not an easy task. It is well known that the addition theorem can be employed to solve this problem [22,23]. However, the addition theorem of Mathieu functions will make the formulation and the corresponding numerical calculation complicated due to its infinite series form. In this paper Eqs. (17) and (18) are calculated without using the addition theorem of Mathieu functions. In order to achieve this, two difficulties must be surmounted. One is the determination of elliptical coordinates with respect to different local coordinate systems. The other is how to calculate the normal derivative of Mathieu functions with respect to different local coordinate systems.

#### 4. The collocation multipole method

In order to avoid the complex application of the addition theorem, the collocation method is adopted to calculate Eqs. (17) and (18) directly in each local elliptical coordinate system. Consider an elliptical cavity with  $H$  elliptical cylinders subject to the sound-hard condition, as shown in Fig. 1. By uniformly collocating  $N$  ( $=2M+1$ ) points on each elliptical boundary and truncating the infinite series of Eq. (18), we have

$$\begin{aligned} \frac{\partial}{\partial n} P(\mathbf{x}; \zeta_1^{gn}, \eta_1^{gn}, \zeta_2^{gn}, \eta_2^{gn}, \dots, \zeta_L^{gn}, \eta_L^{gn}) &= c_0^1 \frac{\partial}{\partial n} (\text{Mc}_0^{(1)}(\zeta_1^{gn}, q) \text{ce}_0(\eta_1^{gn}, q)) \\ &+ \sum_{m=1}^M c_m^1 \frac{\partial}{\partial n} (\text{Mc}_m^{(1)}(\zeta_1^{gn}, q) \text{ce}_m(\eta_1^{gn}, q)) + s_m^1 \frac{\partial}{\partial n} (\text{Ms}_m^{(1)}(\zeta_1^{gn}, q) \text{se}_m(\eta_1^{gn}, q)) \\ &+ \sum_{j=2}^L \left[ c_0^j \frac{\partial}{\partial n} (\text{Mc}_0^{(3)}(\zeta_j^{gn}, q) \text{ce}_0(\eta_j^{gn}, q)) + \sum_{m=1}^M c_m^j \frac{\partial}{\partial n} (\text{Mc}_m^{(3)}(\zeta_j^{gn}, q) \text{ce}_m(\eta_j^{gn}, q)) + s_m^j \frac{\partial}{\partial n} (\text{Ms}_m^{(3)}(\zeta_j^{gn}, q) \text{se}_m(\eta_j^{gn}, q)) \right] \end{aligned} \quad (19)$$

for  $g=1, 2, \dots, L$  and  $n=1, 2, 3, \dots, N$ , where  $\zeta_j^{gn}$  and  $\eta_j^{gn}$  denote elliptical coordinates of the  $n$ th collocation point on the  $g$ th elliptical boundary with respect to the  $j$ th local elliptical coordinate system. A linear algebraic system of  $LN$  equations in  $LN$  unknowns can be written as follows:

$$\begin{bmatrix} \mathbf{A}^{11} & \mathbf{A}^{12} & \dots & \mathbf{A}^{1L} \\ \mathbf{A}^{21} & \mathbf{A}^{22} & \dots & \mathbf{A}^{2L} \\ \vdots & \vdots & \ddots & \vdots \\ \mathbf{A}^{L1} & \mathbf{A}^{L2} & \dots & \mathbf{A}^{LL} \end{bmatrix} \begin{Bmatrix} \mathbf{b}^1 \\ \mathbf{b}^2 \\ \vdots \\ \mathbf{b}^L \end{Bmatrix} = \begin{Bmatrix} \mathbf{0} \\ \mathbf{0} \\ \vdots \\ \mathbf{0} \end{Bmatrix} \quad (20)$$

The explicit expression for sub-vectors  $[\mathbf{b}^j]$  can be described as follows:

$$\mathbf{b}^j = \begin{Bmatrix} c_0^j \\ c_1^j \\ s_1^j \\ \vdots \\ c_M^j \\ s_M^j \end{Bmatrix}, \quad (21)$$

The explicit expression for the sub-matrices of  $A^{gj}$  can be written in the following form:

$$\begin{bmatrix} \frac{\partial}{\partial n} (\text{Mc}_0^{(1)}(\zeta_j^{g1}, q) \text{ce}_0(\eta_j^{g1}, q)) & \frac{\partial}{\partial n} (\text{Mc}_1^{(1)}(\zeta_j^{g1}, q) \text{ce}_1(\eta_j^{g1}, q)) & \dots & \frac{\partial}{\partial n} (\text{Ms}_M^{(1)}(\zeta_j^{g1}, q) \text{se}_M(\eta_j^{g1}, q)) \\ \frac{\partial}{\partial n} (\text{Mc}_0^{(1)}(\zeta_j^{g2}, q) \text{ce}_0(\eta_j^{g2}, q)) & \frac{\partial}{\partial n} (\text{Mc}_1^{(1)}(\zeta_j^{g2}, q) \text{ce}_1(\eta_j^{g2}, q)) & \dots & \frac{\partial}{\partial n} (\text{Ms}_M^{(1)}(\zeta_j^{g2}, q) \text{se}_M(\eta_j^{g2}, q)) \\ \vdots & \vdots & \ddots & \vdots \\ \frac{\partial}{\partial n} (\text{Mc}_0^{(1)}(\zeta_j^{gN}, q) \text{ce}_0(\eta_j^{gN}, q)) & \frac{\partial}{\partial n} (\text{Mc}_1^{(1)}(\zeta_j^{gN}, q) \text{ce}_1(\eta_j^{gN}, q)) & \dots & \frac{\partial}{\partial n} (\text{Ms}_M^{(1)}(\zeta_j^{gN}, q) \text{se}_M(\eta_j^{gN}, q)) \end{bmatrix} \quad (22)$$

for the subscript  $j=1$  and the same expression as Eq. (22) has to be used with Mathieu functions of the third kind for the subscript  $j \neq 1$ .

To calculate  $A^{gj}$  of Eq. (22), two tasks need to be done: one is the determination of elliptical coordinates  $(\zeta_j^{gn}, \eta_j^{gn})$ ,  $n=1, 2, \dots, N$ , of the collocation point with respect to each local elliptical coordinate system. When  $g=j$ , elliptical coordinates,  $(\zeta_g^{gn}, \eta_g^{gn})$ , can be easily determined, being uniformly distributed along the elliptical boundary. On the other hand, when  $g \neq j$ , elliptical coordinates  $(\zeta_j^{gn}, \eta_j^{gn})$  can be determined from  $(\zeta_g^{gn}, \eta_g^{gn})$  through the transformation between two local elliptical systems. First, as shown in Fig. 3, rectangular coordinates in the  $g$ th coordinate system are determined

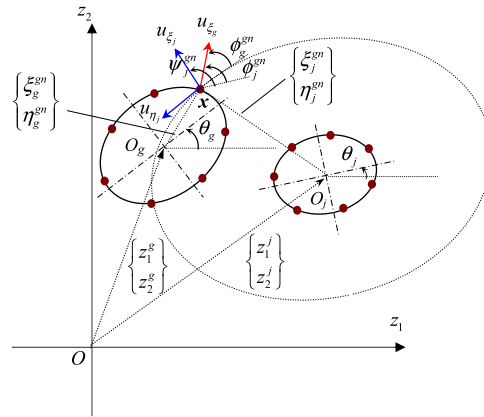


Fig. 3. Collocation point and notation of coordinate transformation.

from the elliptical ones by Eq. (3) as follows:

$$x_g^{gn} + iy_g^{gn} = f \cosh(\zeta_g^{gn} + i\eta_g^{gn}) \tag{23}$$

and then the rectangular coordinates in the *j*th local system can be transformed from the *g*th local system by

$$\begin{Bmatrix} x_j^{gn} \\ y_j^{gn} \end{Bmatrix} = \mathbf{R}(-\theta_j) \left\{ \mathbf{T}(O_j, O_g) + \mathbf{R}(\theta_g) \begin{Bmatrix} x_g^{gn} \\ y_g^{gn} \end{Bmatrix} \right\}, \tag{24}$$

where

$$\mathbf{R}(\theta) = \begin{bmatrix} \cos(\theta) & -\sin(\theta) \\ \sin(\theta) & \cos(\theta) \end{bmatrix} \text{ and } \mathbf{T}(O_j, O_g) = \begin{Bmatrix} z_1^g \\ z_2^g \end{Bmatrix} - \begin{Bmatrix} z_1^j \\ z_2^j \end{Bmatrix}.$$

Finally, the elliptical coordinates with respect to the *j*th elliptical coordinate system are determined by

$$\zeta_j^{gn} + i\eta_j^{gn} = \cosh^{-1} \left( \frac{x_j^{gn} + iy_j^{gn}}{f} \right). \tag{25}$$

By this way, the elliptical coordinates of collocation points with respect to any local elliptical coordinate system can be easily determined.

The other task is the gradient calculation in  $A^{gj}$ . When  $g=j$ , the element of  $A^{gg}$  can be easily determined, for example at the *n*th collocation point on the *g*th boundary, by

$$\frac{\partial}{\partial n} (\text{Mc}_m^{(1)}(\zeta, q) \text{ce}_m(\eta, q)) = \text{ce}_m(\eta, q) \frac{\partial \text{Mc}_m^{(1)}(\zeta, q)}{h_\zeta \partial \zeta} \Big|_{\zeta = \zeta_g^{gn}, \eta = \eta_g^{gn}}. \tag{26}$$

On the other hand, when  $g \neq j$ , it can be done by directional derivative. Before that, the angle of the vector normal to elliptical boundary at collocation point with respect to each local coordinate system must be determined. When  $g=j$ , the angle  $\phi_g^{gn}$  (the definition of the subscript or superscript are same as  $\zeta_g^{gn}$ ), as shown in Fig. 3, can be determined by

$$\phi_g^{gn} = \tan^{-1} \left( \frac{\tan \eta_g^{gn}}{\tanh \zeta_g^{gn}} \right). \tag{27}$$

When  $g \neq j$ , the angle  $\phi_j^{gn}$ , as shown in Fig. 3, is defined by

$$\phi_j^{gn} = \phi_g^{gn} + \theta_g - \theta_j, \tag{28}$$

where  $\theta_g$  and  $\theta_j$  are orientation angles of the *g*th and the *j*th local coordinate system. When  $g \neq j$ , the derivative normal to the *g*th boundary with respect to the *j*th local elliptical coordinate system is determined by

$$\frac{\partial B}{\partial n} = \nabla B_j \cdot n = \left[ \frac{\partial B}{h_\zeta \partial \zeta_j} \quad \frac{\partial B}{h_\eta \partial \eta_j} \right] \begin{bmatrix} \cos \delta \\ \sin \delta \end{bmatrix} = \left( \frac{\partial B}{h_\zeta \partial \zeta_j} \right) \cos \delta + \left( \frac{\partial B}{h_\eta \partial \eta_j} \right) \sin \delta, \tag{29}$$

where  $B$  may be either one of  $\text{Mc}_m^{(1)}(\xi, q)\text{ce}_m(\eta, q)$ ,  $\text{Mc}_m^{(3)}(\xi, q)\text{ce}_m(\eta, q)$ ,  $\text{Ms}_m^{(1)}(\xi, q)\text{se}_m(\eta, q)$  and  $\text{Ms}_m^{(3)}(\xi, q)\text{se}_m(\eta, q)$  and  $h_\xi = h_\eta$ . The parameter  $\delta$  in Eq. (29) is defined by

$$\delta = \phi_j^{gn} - \psi_j^{gn}, \tag{30}$$

where  $\psi_j^{gn}$  is the angle of the unit vector normal to the curves of  $\xi = \text{constant}$ ,  $u_{\xi_j}$ , as shown in Fig. 3 (the definition of the subscript or superscript are same as  $\xi_j^{gn}$ ), defined by

$$\psi_j^{gn} = \tan^{-1} \left( \frac{\tan \eta_j^{gn}}{\tanh \xi_j^{gn}} \right). \tag{31}$$

In general,  $\partial/\partial n(\text{Mc}_m^{(1)}(\xi, q)\text{ce}_m(\eta, q))$  at  $(\xi_j^{gn}, \eta_j^{gn})$  can be explicitly expressed as

$$\left( \text{ce}_m(\eta, q) \frac{\partial \text{Mc}_m^{(1)}(\xi, q)}{h_\xi \partial \xi} \right) \cos \delta + \left( \text{Mc}_m^{(1)}(\xi, q) \frac{\partial \text{ce}_m(\eta, q)}{h_\eta \partial \eta} \right) \sin \delta \Big|_{\xi = \xi_j^{gn}, \eta = \eta_j^{gn}}. \tag{32}$$

Finally, the normal derivative with respect to any local elliptical coordinate system can be exactly calculated without any truncation problem which inevitably occurred in using the addition theorem. When  $g=j$  in Eq. (31),  $\psi_g^{gn}$  equals to  $\phi_g^{gn}$ , the parameter  $\delta$  becomes zero and then Eq. (32) reduces to Eq. (26).

After determining the element of the linear algebraic system, based on the direct-searching scheme [24], the natural frequencies are determined by detecting the drop of the minimum singular value of Eq. (20) by performing a frequency sweep. In our approach, two steps are employed. In the first step, a larger frequency interval  $\Delta k$  is taken. For example, the value of 0.01 is chosen to sweep the frequency range of our concern. For the second step, a local sweep with a smaller frequency step is applied depending on the precision requirement of the considered problem. For instance, the value of 0.0001 is adopted in this paper. That is to say that an adaptive  $\Delta k$  scheme is used. Once the eigenvalues are found, the associated mode shapes can be obtained by substituting the corresponding eigenvectors (i.e. the coefficients of the multipole expansion) into the multipole expansion for the acoustic pressure, Eq. (17).

### 5. Numerical results and discussions

To demonstrate the validity of the proposed method, a FORTRAN code was implemented to determine natural frequencies and modes of an acoustic cavity with multiple elliptical boundaries, using the subroutines of the Mathieu function provided by Zhang and Jin [10]. For the simple geometries such as an elliptical cavity or a confocal elliptical annulus cavity, the analytical eigensolutions were derived and used to verify the proposed method. The same problem was independently solved by using the commercial finite-element code ABAQUS [25] for comparison. The acoustic elements of type AC2D3 were employed to model the acoustic cavity. In all cases, the boundaries are subject to the sound-hard or Neumann boundary conditions and  $c$  is assumed to be one, that is, the wavenumber equals to the natural radian frequency in the following numerical examples.

#### Case 1. An elliptical cavity

The sound-hard boundary condition of an elliptical cavity gives

$$\frac{\partial P(\xi, q)}{\partial \xi} \Big|_{\xi = \xi_1} = 0. \tag{33}$$

Substituting Eq. (15) into Eq. (33) yields

$$\sum_{m=0}^{\infty} c_m \text{ce}_m(\eta, q) \frac{\partial \text{Mc}_m^{(1)}(\xi, q)}{\partial \xi} + s_m \text{se}_m(\eta, q) \frac{\partial \text{Ms}_m^{(1)}(\xi, q)}{\partial \xi} \Big|_{\xi = \xi_1} = 0 \tag{34}$$

for  $0 \leq \eta < 2\pi$ . To obtain the nontrivial solution for the coefficients  $c_m$  and  $s_m$ , we have

$$\frac{\partial \text{Mc}_m^{(1)}(\xi, q)}{\partial \xi} \Big|_{\xi = \xi_1} = 0, \quad m = 0, 1, 2, \dots \tag{35}$$

for even modes and

$$\frac{\partial \text{Ms}_m^{(1)}(\xi, q)}{\partial \xi} \Big|_{\xi = \xi_1} = 0, \quad m = 1, 2, \dots \tag{36}$$

for odd modes, which are the characteristic equations, their solutions giving the eigenvalues.

A numerical example of an elliptical cavity with  $a=1.0$  and  $b=0.5$  as shown in Fig. 4 is first considered where the radial coordinate of its boundary  $\xi_1$  is constant, being 0.5493 and the interfocal distance  $2f$  is 1.732. Figs. 5 and 6 are plots of the left hand side functions of Eqs. (35) and (36). Since  $f$  and  $\xi_1$  are given, instead of the parameter  $q$ , the wavenumber  $k$  is used as the  $x$ -axis and zeros of these functions,  $k_{eij}$  shown in Fig. 5 and  $k_{oij}$  in Fig. 6, indicate the even and the odd eigenvalues, respectively. The subscript denotes the mode type defined as follows: the first parameters,  $e$  and  $o$ , denote the mode shape

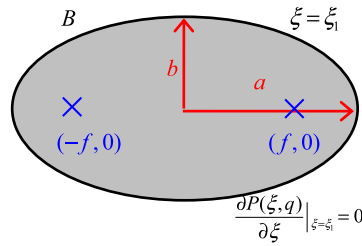


Fig. 4. An elliptical cavity.

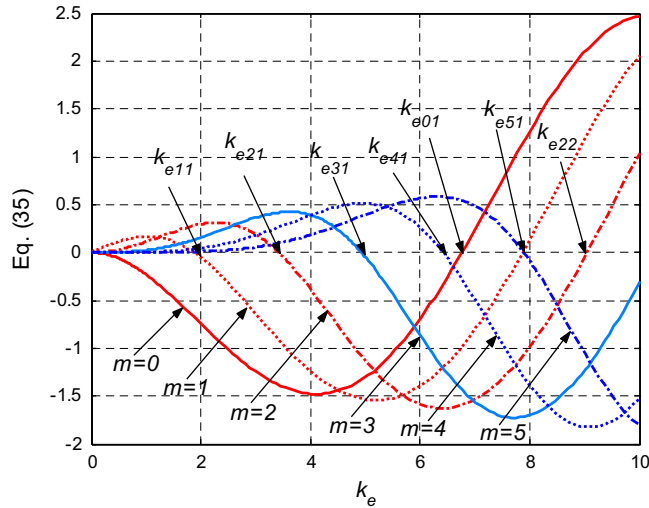


Fig. 5. Zeros of the characteristic equation of even modes for an elliptical cavity.

having symmetry and anti-symmetry with respect to the major axis, respectively, the second parameter denotes the order of Mathieu functions, equaling to the number of nodal line, which can be seen from the following mode shapes, and the third one, for example  $j$ , denotes the  $j$ th zero of the characteristic equation. The lower eight natural modes versus the number of coefficients of the multipole expansion for this case are shown in Fig. 7 where the mode type is in parentheses. From this convergence analysis, the required number of coefficients,  $M$ , just equals to the number of nodal line of the corresponding natural mode due to its analytical nature. It demonstrates that the present method has a high rate of convergence. Consequently, only four coefficients ( $M=4$ ) is sufficient to capture the lower eight modes. It can be seen from numerical results that the number of coefficients used will only influence the number of mode appeared, but the value of natural frequency of the captured mode can be well predicted. Fig. 8 shows the minimum singular values of the influence matrix of Eq. (20) versus the wavenumber  $k$ . Since the direct-searching scheme is used, the drop location indicates possible eigenvalues, for example 1.6736 being the first natural mode. From viewing Figs. 5, 6 and 8, the drop locations of Fig. 8 agree with zeros of the characteristic equations of Figs. 5 and 6. No spurious eigenvalues are found in the proposed results since a complete basis is employed in our formulation, leading to a full-rank linear algebra system.

For this case, the 6604 elements and 3403 nodes were used to generate the FEM model and solved the same problem. Fig. 9 shows the lower seven natural modes by using the present method, the FEM and the analytical method and indicates good agreements. The dashed line denotes the nodal line and, as mentioned previously, its number equals to the order for the Mathieu functions. Numerical results show that the natural frequencies of the present method match better with those of the analytical method than those of the ABAQUS. After comparing with the mesh size of the FEM model, the computational efficiency and convergence of the present method over the FEM is evident.

**Case 2. A confocal elliptical annulus cavity**

The sound-hard boundary condition of a confocal elliptical annulus cavity gives

$$\frac{\partial P(\xi, q)}{\partial \xi} \Big|_{\xi=\xi_1} = 0 \text{ and } \frac{\partial P(\xi, q)}{\partial \xi} \Big|_{\xi=\xi_2} = 0 \tag{37}$$



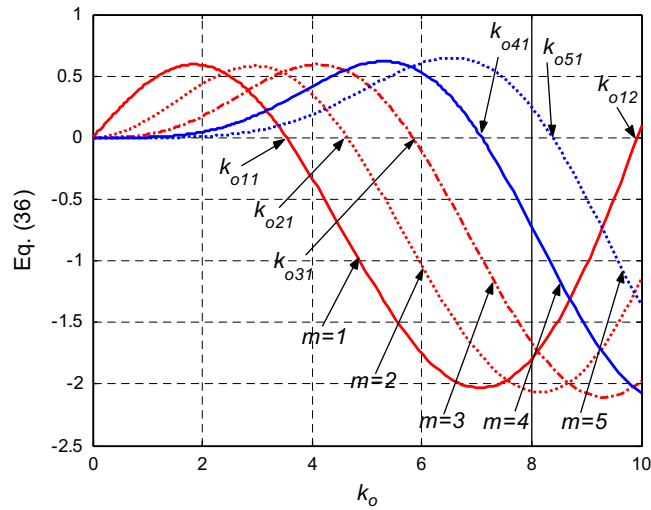


Fig. 6. Zeros of the characteristic equation of odd modes for an elliptical cavity.

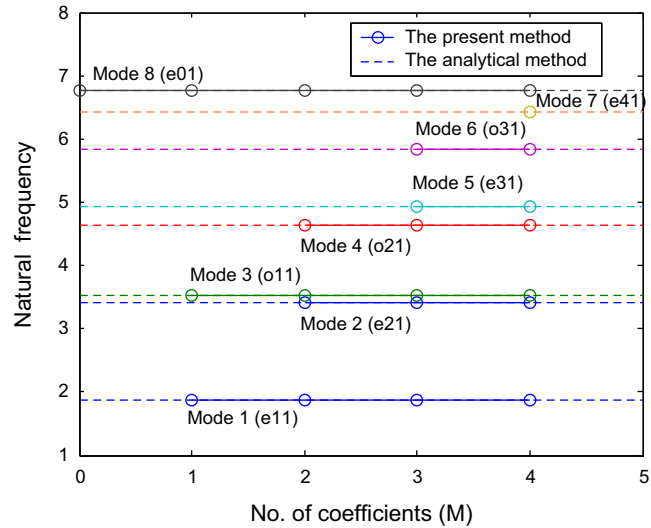


Fig. 7. The lower eight natural modes versus the number of coefficients of the multipole expansion for an elliptical cavity.

Substituting Eq. (17) with  $L=2$  into Eq. (37) and recollecting the terms yield

$$\begin{bmatrix} \frac{\partial}{\partial \xi} \text{Mc}_m^{(1)}(\xi_1, q) & \frac{\partial}{\partial \xi} \text{Mc}_m^{(3)}(\xi_1, q) \\ \frac{\partial}{\partial \xi} \text{Mc}_m^{(1)}(\xi_2, q) & \frac{\partial}{\partial \xi} \text{Mc}_m^{(3)}(\xi_2, q) \end{bmatrix} \begin{Bmatrix} c_m^1 \\ c_m^2 \end{Bmatrix} = \begin{Bmatrix} 0 \\ 0 \end{Bmatrix}, \quad m = 0, 1, 2, \dots \quad (38)$$

and

$$\begin{bmatrix} \frac{\partial}{\partial \xi} \text{Ms}_m^{(1)}(\xi_1, q) & \frac{\partial}{\partial \xi} \text{Ms}_m^{(3)}(\xi_1, q) \\ \frac{\partial}{\partial \xi} \text{Ms}_m^{(1)}(\xi_2, q) & \frac{\partial}{\partial \xi} \text{Ms}_m^{(3)}(\xi_2, q) \end{bmatrix} \begin{Bmatrix} s_m^1 \\ s_m^2 \end{Bmatrix} = \begin{Bmatrix} 0 \\ 0 \end{Bmatrix}, \quad m = 1, 2, \dots \quad (39)$$

for  $0 \leq \eta < 2\pi$ . To obtain the nontrivial solution for the coefficients  $c_m^1, c_m^2, s_m^1$  and  $s_m^2$ , separating real and imaginary parts of Eqs. (38) and (39) gives

$$\frac{\partial}{\partial \xi} \text{Mc}_m^{(1)}(\xi_1, q) \frac{\partial}{\partial \xi} \text{Mc}_m^{(2)}(\xi_2, q) - \frac{\partial}{\partial \xi} \text{Mc}_m^{(2)}(\xi_1, q) \frac{\partial}{\partial \xi} \text{Mc}_m^{(1)}(\xi_2, q) = 0, \quad m = 0, 1, 2, \dots \quad (40)$$

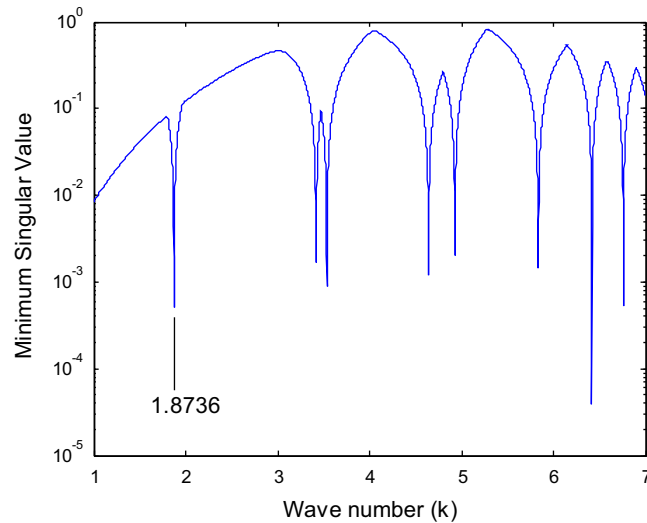


Fig. 8. The minimum singular value  $\sigma_1$  versus  $k$  for an elliptical cavity.

Mode No.	1	2	3	4	5	6	7
Mode type	e11	e21	o11	o21	e31	o31	e41
The present Method	1.8736	3.4190	3.5354	4.6412	4.9291	5.8352	6.4180
ABAQUS (No. of elements =6604)	1.8737	3.4188	3.5347	4.6395	4.9275	5.8317	6.4139
$k$ (Analytical method)	1.8736	3.4191	3.5355	4.6414	4.9292	5.8354	6.4182

Fig. 9. The lower seven natural modes for an elliptical cavity by using the present method, the FEM and the analytical method.

for even mode and

$$\frac{\partial}{\partial \xi} Ms_m^{(1)}(\xi_1, q) \frac{\partial}{\partial \xi} Ms_m^{(2)}(\xi_2, q) - \frac{\partial}{\partial \xi} Ms_m^{(2)}(\xi_1, q) \frac{\partial}{\partial \xi} Ms_m^{(1)}(\xi_2, q) = 0, \quad m = 1, 2, \dots \tag{41}$$

for odd mode, which are the characteristic equations, zeros of these equations giving the eigenvalues.

A numerical example of a confocal elliptical annulus cavity with  $a_1 = 1.4434$ ,  $b_1 = 1.1547$ ,  $a_2 = 1.0$  and  $b_2 = 0.5$  as shown in Fig. 10 is presented where the interfocal distance  $2f$  is 1.732, and the radial coordinates of the outer and the inner ellipse,  $\xi_1$  and  $\xi_2$ , are 1.0986 and 0.5493, respectively. Figs. 11 and 12 are plots of the characteristic equations of Eqs. (40) and (41) and zeros of these equations provide the analytical eigenvalues. Fig. 13 presents the lower eight natural modes versus the number of coefficients and still shows fast-rate convergence for this case. It indicates that the appearance of the predicted mode depends only on the number of coefficients, which equals to that of the nodal line or the order of the Mathieu function. Fig. 14 shows the minimum singular values of the influence matrix of Eq. (20) versus the wavenumber  $k$ . For this case, the 15 548 elements and 8045 nodes were used to generate the FEM model. Fig. 15 shows the lower seven natural modes by using the present method, the FEM and the analytical method and indicates good agreements.

**Case 3.** An elliptical cavity with two elliptical cylinders

In order to demonstrate the generality of the present method, an elliptical cavity with two elliptical cylinders is considered as shown in Fig. 16, where  $a_1 = 1.4$ ,  $b_1 = 1.1$ ,  $a_2 = 0.3$ ,  $b_2 = 0.2$ ,  $a_3 = 0.4$  and  $b_3 = 0.2$ . The center coordinates of the two elliptical cylinders are (0.7, 0) and (-0.4, 0.3), respectively, with respect to the center of outer ellipse. The angle of orientation of the two elliptical cylinders are  $\pi/6$  and 0, respectively. Unlike the previous cases, the closed-form characteristic equation for this case is not available due to its complicated geometry. The same problem is also solved by using the FEM (ABAQUS) and its model needs 18 903 elements in order to obtain acceptable results for comparison. Fig. 17 shows the lower seven natural modes versus the number of coefficients of the multipole expansion where the

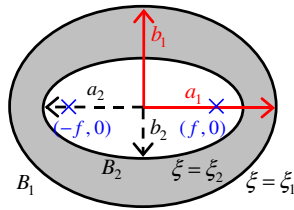


Fig. 10. A confocal elliptical annulus cavity.

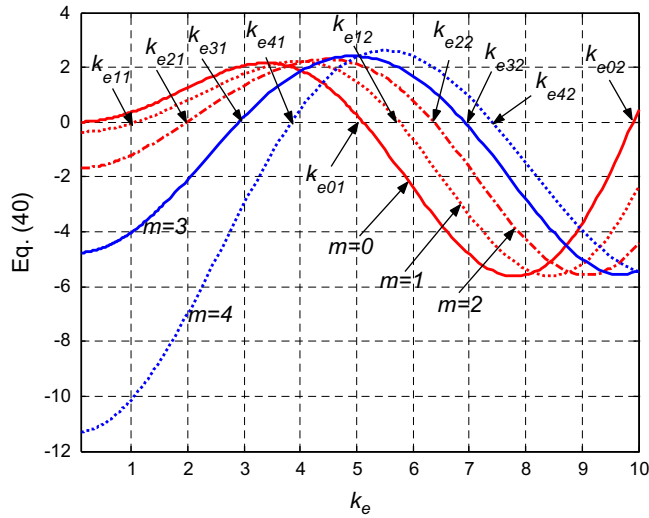


Fig. 11. Zeros of the characteristic equation of even modes for a confocal elliptical annulus cavity.

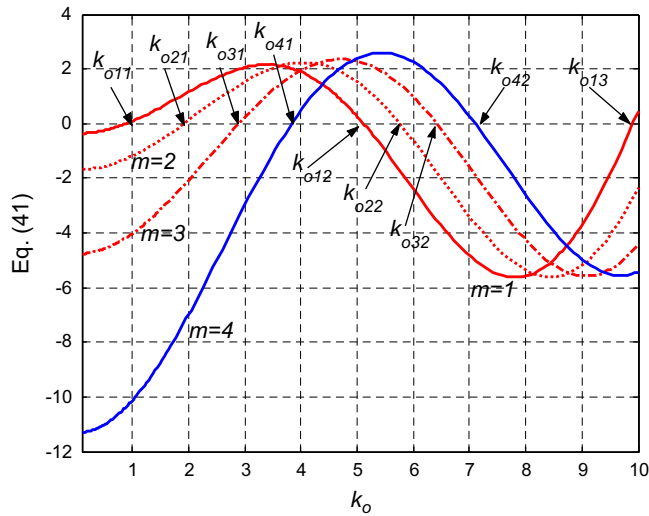


Fig. 12. Zeros of the characteristic equation of odd modes for a confocal elliptical annulus cavity.

dashed line denotes the results provided by the FEM. Not only the accuracy of predicted eigenvalues but also the appearance of their corresponding modes depends on the number of coefficients used. Specifically, the more the number of coefficients is, the more accurate the natural frequency is. From the convergence analysis, five coefficients are enough to capture the lower seven natural modes. It shows that the convergence of the present method is still fast even for this complicated configuration. Due to the complicated form of the addition theorem for the Mathieu functions, the corresponding convergence results for this case are not available in the literature. But the convergence results for those

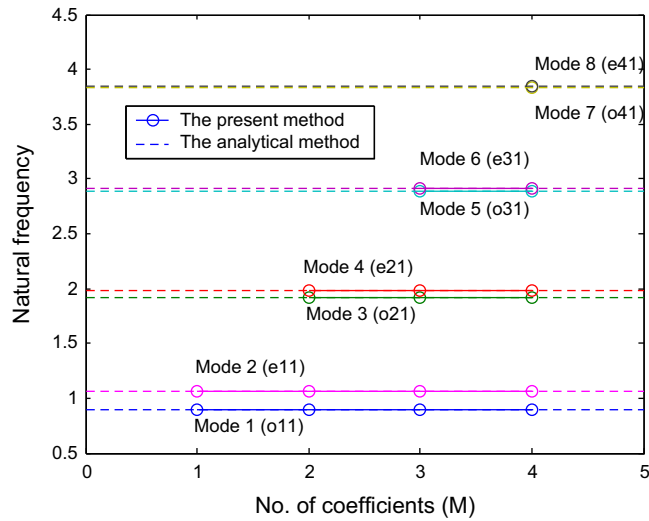


Fig. 13. The lower eight natural modes versus the number of coefficients of the multipole expansion for a confocal elliptical annulus cavity.

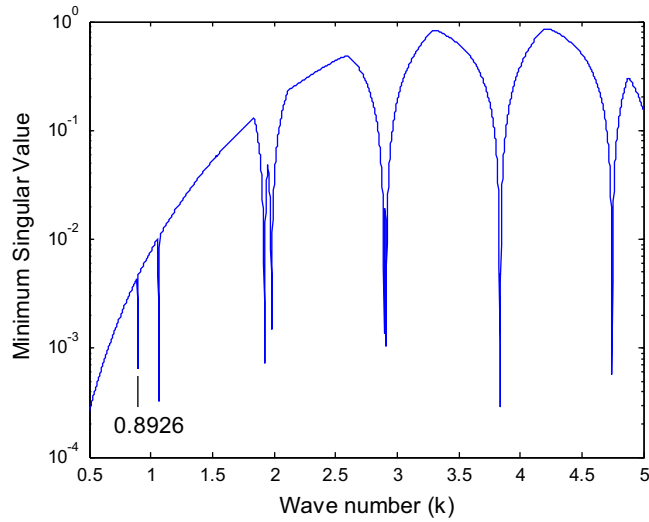


Fig. 14. The minimum singular value  $\sigma_1$  versus  $k$  for a confocal elliptical annulus cavity.

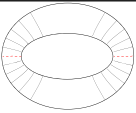
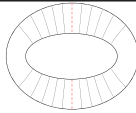
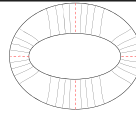
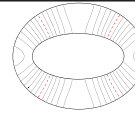
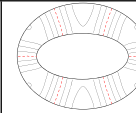
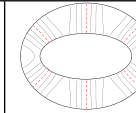
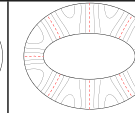
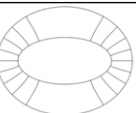
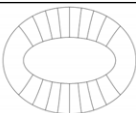
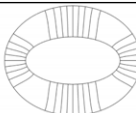
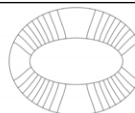
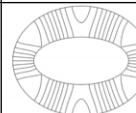
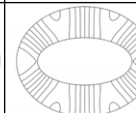
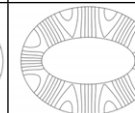
Mode No.	1	2	3	4	5	6	7
Mode type	o11	e11	o21	e21	o31	e31	o41
The present Method	0.8926	1.0643	1.9216	1.9809	2.8947	2.9135	3.8345
							
ABAQUS (No. of elements =15548)	0.8928	1.0643	1.9218	1.9809	2.8946	2.9133	3.8339
							
$k$ (Analytical method)	0.8926	1.0644	1.9216	1.9810	2.8948	2.9136	3.8347

Fig. 15. The lower seven natural modes for a confocal elliptical annulus cavity by using the present method, the FEM and the analytical method.

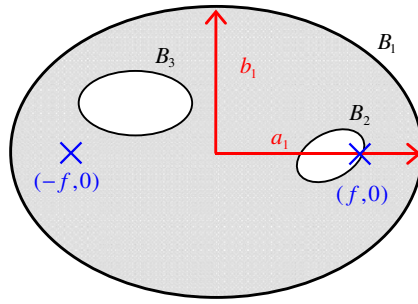


Fig. 16. An elliptical cavity with two elliptical cylinders.

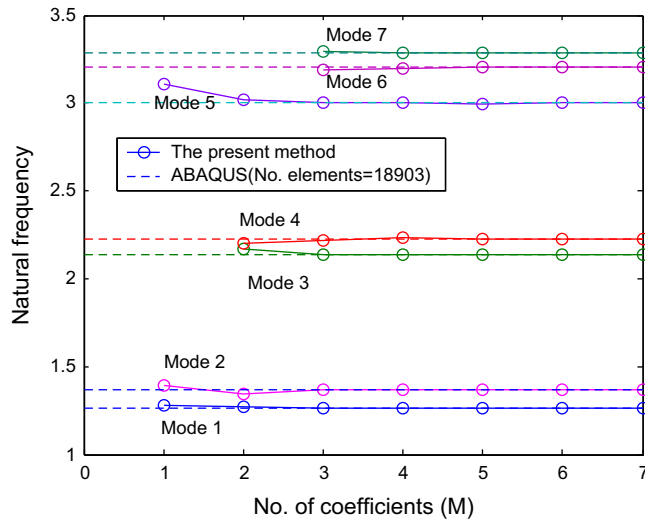


Fig. 17. The lower seven natural modes versus the number of coefficients of the multipole expansion for an elliptical cavity with two elliptical cylinders.

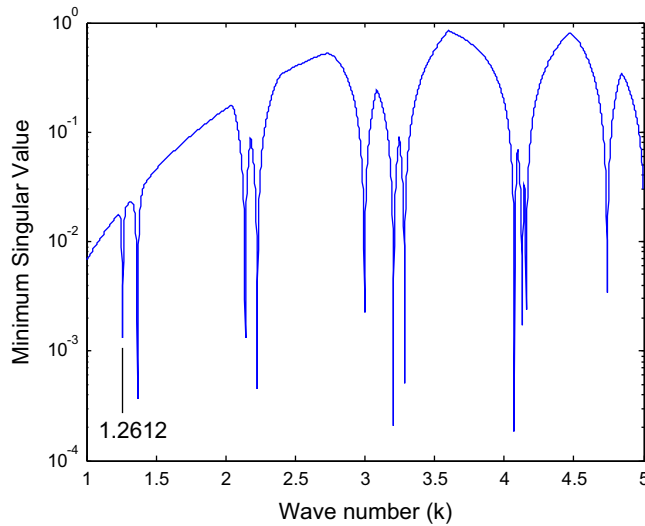


Fig. 18. The minimum singular value  $\sigma_1$  versus  $k$  for an elliptical cavity with two elliptical cylinders.

with circular boundaries, using the addition theorem of the Bessel functions, can be found in Ref. [20]. It shows that the two approaches have fast rate of convergence. However, the present method is clear in formulation and applicable in practice. By using six coefficients ( $M=6$ ), the minimum singular values of the influence matrix of Eq. (20) versus the

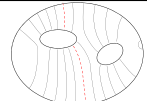
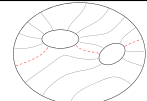
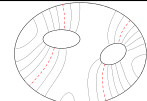
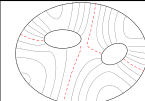
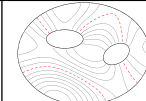
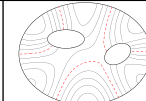
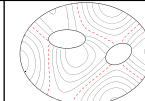


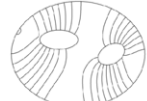




Mode No.	1	2	3	4	5	6	7
The present Method	1.2612	1.3674	2.1389	2.2281	2.9985	3.2032	3.2843
							
ABAQUS (No. of elements =18903)	1.2613	1.3684	2.1395	2.2286	2.9985	3.2033	3.2842
							

Fig. 19. The lower seven natural modes for an elliptical cavity with two elliptical cylinders by using the present method and the FEM.

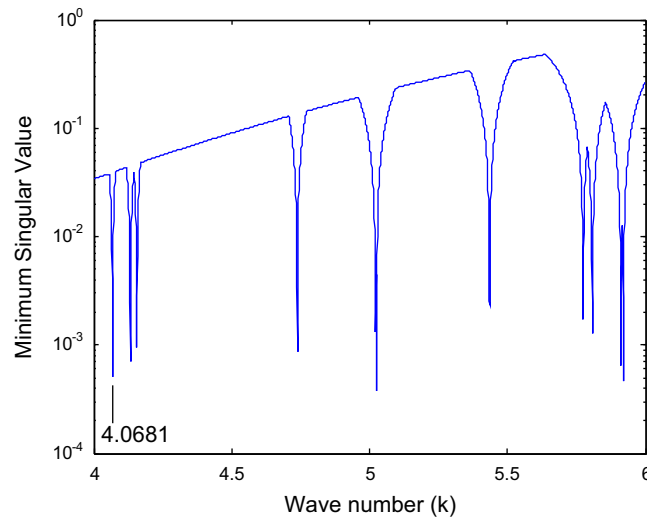


Fig. 20. The minimum singular value  $\sigma_1$  of the higher modes versus  $k$  for an elliptical cavity with two elliptical cylinders.

Table 1

The higher eigenvalues of an elliptical cavity with two elliptical cylinders by using the present method and FEM.

Eigenvalue	Present method	FEM(ABAQUS)		
		19 739 nodes	9689 nodes	4337 nodes
$K_8$	4.0681	4.0678	4.0675	4.0666
$K_9$	4.1328	4.1324	4.1320	4.1310
$K_{10}$	4.1563	4.1559	4.1555	4.1546
$K_{11}$	4.7378	4.7372	4.7366	4.7349
$K_{12}$	5.0216	5.0207	5.0198	5.0175
$K_{13}$	5.0249	5.0240	5.0231	5.0206
$K_{14}$	5.4355	5.4343	5.4331	5.4301
$K_{15}$	5.7744	5.7732	5.7720	5.7690
$K_{16}$	5.8077	5.8060	5.8041	5.7999
$K_{17}$	5.9118	5.9101	5.9085	5.9038

wavenumber  $k$  is shown in Fig. 18. Fig. 19 shows the lower seven natural modes by using the present method and the FEM. Excellent agreement between the results of the present method and those of the ABAQUS is observed.

To further illustrate the performance of the present method in the high frequency range, the next ten, the 8th–17th, natural frequencies are determined by using the proposed method and FEM for comparison. To calculate the higher natural frequencies, more coefficients ( $M=10$ ) should be used to obtain accurate results. Fig. 20 shows the minimum singular values of the higher modes versus the wavenumber  $k$ , where the troughs indicate eigenvalues such as the 8th natural

frequency 4.0681. Table 1 summarizes the 8th–17th natural frequencies of the present method and FEM. In comparison to the results provided by various finite element meshes, the present results show excellent accuracy.

## 6. Conclusions

A semi-analytical approach has been proposed and successfully applied to solve the eigenproblem of an acoustic cavity with multiple elliptical boundaries. Natural frequencies and modes are determined by using the multipole method, the coordinate transformation, the directional derivative and the singular value decomposition (SVD). Instead of using the addition theorem, the calculation of the multipole expansion is directly calculated in each coordinate system when considering problems with a multiply-connected domain. The proposed algorithm is easily applicable to the problem with multiple elliptical boundaries free of the complicated formulation and associated numerical calculation caused by the addition theorem of Mathieu functions. For the simple geometries such as an elliptical cavity and a confocal elliptical annulus cavity, the results from the proposed methodology agree with those of the analytical method. For the complicated case of an elliptical cavity with two elliptical cylinders, the proposed results match well with those of the finite element method by using the ABAQUS code where a lot of elements were required to obtain acceptable solutions for comparison. It follows from several numerical experiments that the proposed formulation does not yield spurious eigenvalues. Numerical results demonstrate that the present method has good accuracy and fast rate of convergence. It may be worth mentioning that the proposed method can be extended to the 3D cavities or exterior (or scattering) problems without any difficulties. They are among our further research goals.

## Acknowledgements

Financial support from the National Science Council under the Grant No. NSC 99-2221-E-157-003- for China University of Science and Technology is gratefully appreciated.

## References

- [1] K. Hong, J. Kim, Natural mode analysis of hollow and annular elliptical cylindrical cavities, *Journal of Sound and Vibration* 183 (2) (1995) 327–351.
- [2] I.L. Chen, J.T. Chen, S.R. Kuo, M.T. Liang, A new method for true and spurious eigensolutions of arbitrary cavities using the combined Helmholtz exterior integral equation formulation method, *Journal of Acoustical Society of America* 109 (3) (2001) 982–998.
- [3] M.K. Au-Yang, Pump induced acoustic pressure distributed in an annular cavity bounded by rigid walls, *Journal of Sound and Vibration* 62 (1979) 577–591.
- [4] J. Kim, W. Soedel, General formulation of four pole parameters for three dimensional cavities utilizing modal expansion with special attention to the annular cylinder, *Journal of Sound and Vibration* 129 (1989) 237–254.
- [5] J.T. Chen, L.W. Liu, H.K. Hong, Spurious and true eigensolutions of Helmholtz BIEs and BEMs for a multiply-connected problem, *Proceedings of the Royal Society of London, Series A* 459 (2003) 1891–1925.
- [6] J.T. Chen, C.T. Chen, I.L. Chen, Null-field integral equation approach for eigenproblems with circular boundaries, *Journal of Computational Acoustics* 15 (4) (2007) 401–428.
- [7] N.W. McLachlan, *Theory and Application of Mathieu Functions*, University Press, Oxford, 1947.
- [8] M. Abramowitz, I.A. Stegun, *Handbook of Mathematical Functions*, Dover, New York, 1965.
- [9] Y.H. Pao, C.C. Mow, *Diffraction of Elastic Waves and Dynamics Stress Concentration*, Crane-Russak, New York, 1972.
- [10] S. Zhang, J. Jin, *Computation of Special Functions*, John Wiley, New York, 1996.
- [11] J.C. Gutierrez-Vega, R.M. Rodriguez-Dagnino, M.A. Meneses-Nava, S. Chavez-Cerda, Mathieu functions, a visual approach, *American Journal of Physics* 71 (3) (2003) 233–241.
- [12] I.S. Gradshteyn, I.M. Ryzhik, *Table of Integrals, Series, and Products*, 7th edition, Academic Press, 2007.
- [13] J.T. Chen, Y.T. Lee, J.W. Lee, Torsional rigidity of a bar with multiple elliptical inclusions using a null-field integral approach, *Computational Mechanics* 46 (2010) 511–519.
- [14] J.T. Chen, J.W. Lee, S.Y. Leu, Analytical investigation for spurious eigen solutions of multiply-connected membranes containing elliptical boundaries using the dual BIEM, *International Journal of Solids and Structures* 48 (2011) 729–744.
- [15] F. Závřiska, Über die Beugung elektromagnetischer Wellen an parallelen, unendlich langen Kreiszyllindern (About the diffraction of electromagnetic waves in parallel, infinitely long circular cylinder), *Annalen der Physik (Annals of physics)* 40 (4) (1913) 1023–1056.
- [16] C.M. Linton, D.V. Evans, The interaction of waves with arrays of vertical circular cylinders, *Journal of Fluid Mechanics* 215 (1990) 549–569.
- [17] P.A. Martin, *Multiple Scattering Interaction of Time-harmonic Wave with N Obstacles*, Cambridge University Press, Cambridge, 2006.
- [18] J.T. Chen, S.K. Kao, W.M. Lee, Y.T. Lee, Eigensolutions of the Helmholtz equation for a multiply-connected domain with circular boundaries by using the multipole Trefftz method, *Engineering Analysis with Boundary Elements* 34 (2010) 463–470.
- [19] E.I. Martynenko, Natural modes of circular membranes and plates weakened by a finite number of circular holes, *International Applied Mechanics* 6 (11) (1970) 1222–1226.
- [20] W.M. Lee, J.T. Chen, Free vibration analysis of a circular plate with multiple circular holes by using the multipole Trefftz method, *Computer Modeling in Engineering & Science* 50 (2) (2009) 141–159.
- [21] W.M. Lee, J.T. Chen, Scattering of flexural wave in thin plate with multiple circular holes by using the multipole Trefftz method, *International Journal of Solids and Structures* 47 (2010) 1118–1129.
- [22] I.K. Chatjigeorgiou, S.A. Mavrakos, Hydrodynamic diffraction by multiple elliptical cylinders, 24th IWWWFB, Zelenogorsk, Russia 2009.
- [23] I.K. Chatjigeorgiou, S.A. Mavrakos, An analytical approach for the solution of the hydrodynamic diffraction by arrays of elliptical cylinders, *Applied Ocean Research* 32 (2010) 242–251.
- [24] M. Kitahara, *Boundary Integral Equation Methods in Eigenvalue Problems of Elastodynamics and Thin Plates*, Elsevier, Amsterdam, 1985.
- [25] ABAQUS 6.5, Hibbit, Karlsson and Sorensen, Inc., RI, 2004.